Phonon thermodynamics versus electron-phonon models

Marco Zoli*
Istituto Nazionale Fisica della Materia, Dipartimento di Fisica, Universitá di Camerino, Camerino 62032, Italy
(Received 18 February 2004; revised manuscript received 1 June 2004; published 15 November 2004)

Applying the path integral formalism we study the equilibrium thermodynamics of the phonon field both in the Holstein and in the Su-Schrieffer-Heeger models. The anharmonic cumulant series, dependent on the peculiar source currents of the e-ph models, have been computed versus temperature in the case of a low energy oscillator. The cutoff in the series expansion has been determined, in the low T limit, using the constraint of the third law of thermodynamics. In the Holstein model, the free energy derivatives do not show any contribution ascribable to the e-ph anharmonic effect. We find signatures of large e-ph anharmonicities in the Su-Schrieffer-Heeger model mainly visible in the temperature dependent peak displayed by the phonon heat capacity.

DOI: 10.1103/PhysRevB.70.184301 PACS number(s): 65.40.−b, 31.15.Kb, 63.20.Ry

I. INTRODUCTION

The equilibrium thermodynamical properties of real systems provide signatures of phonon anharmonicities induced both by electron-phonon and phonon-phonon interactions. While in general the exact thermodynamics of anharmonic e-ph model Hamiltonians can be derived only in one dimension and in the classical limit, variational methods based on the Bogoliubov's inequality[1] permit to obtain (i) upper bounds for the partition functions[2] and (ii) a correct estimate of the entropy within the harmonic theory once the harmonic phonons are self-consistently replaced by the temperature dependent phonon frequencies.[3] Such a replacement however does not hold for other thermodynamic functions and constant volume anharmonic effects have to be explicitly computed by diagrammatic perturbative methods.[4,5] As at high temperatures phonon-phonon anharmonicities are large, in the intermediate to low temperature range the e-ph coupling strength may induce the dominant anharmonic effects in the phonon subsystem, the latter being dependent on the peculiarities of the e-ph model Hamiltonian.

The Holstein Hamiltonian[6] and the Su-Schriffer-Heeger Hamiltonian[7] have been widely investigated in the last decades also in view of the growing interest for polaronic mechanisms in high T_c superconductors[8] and polymers.[9] While the Holstein model assumes a local coupling of tight binding electrons to optical phonons, in the SSH model the electron-phonon interaction modifies the electron hopping matrix elements thus leading to a nonlocal (in momentum space) coupling with vertex function dependent on both the electron and the phonon wave vector.[10,11] As the ground state of the SSH Hamiltonian is twofold degenerate localized solitonic solutions appear in the system together with polarons[12,13] whose formation depends however on the strength of the electron coupling to the induced lattice deformation[14] and on the value of the adiabatic parameter.[15]

Analysis of the Holstein and SSH Hamiltonians generally assume harmonic phonon models although lattice anharmonicities may induce relevant microscopic effects such as the reduction of the Holstein polaron effective mass[16] along with a consistent broadening of the polaron size.[17] In large polaron transport models based on the Holstein Hamiltonian, the effects of the phonon spectrum renormalization on the polaron scattering have been studied both for the optical[18] and the acoustical[19] branches. Phonon anharmonicities have been also proposed as a fundamental feature favoring high T_c superconductivity in the context of (bi)polaronic theories.[20–22]

When the electron energy scale, set by the value of the tight binding overlap integral, is larger of (or comparable to) the characteristic phonon energy the lattice deformation does not follow instantaneously the electron motion[23] and the e-ph interaction becomes time dependent. The path integral formalism[24] is suitable to account for time dependent interactions as a retarded potential naturally emerges in the exact integral action.[25] Moreover, being valid for any e-ph coupling value, the path integral method allows one to derive the partition function and the related temperature derivatives without those limitations which affect the perturbative studies.

Our previous investigations have focused on the equilibrium thermodynamics of the SSH model by assuming a bath of *harmonic* phonons for the electron particle path[26] while anharmonic corrections to the phonon free energy had been only partially considered[27] in the case of a time averaged electron particle path. However, being the e-ph SSH interaction intrinsically nonlocal on the time scale, significant phonon anharmonicities may be found through a full computation of the cumulant expansion depending on the perturbing source current of the Hamiltonian model. With the present paper we propose a comparative analysis of the equilibrium thermodynamics for the phonon system in the Holstein and SSH models pointing out the appearance of macroscopic anharmonic features driven by the strength of the e-ph coupling. In Sec. II we outline the Hamiltonian models and the cumulant expansion for the phonon partition function. The results are presented in Sec. III, while Sec. IV contains some final remarks.

II. THE HAMILTONIAN MODELS

In one dimension the e-ph Holstein Hamiltonian (H^H) and the e-ph SSH Hamiltonian (H^{SSH}) read respectively,

$$H^H = -\frac{J}{2}\sum_r (f_r^\dagger f_{r+1} + f_{r+1}^\dagger f_r) + g\sum_r f_r^\dagger f_r (b_r^\dagger + b_r),$$

$$H^{\mathrm{SSH}} = \sum_r J_{r,r+1}(f_r^\dagger f_{r+1} + f_{r+1}^\dagger f_r),$$

$$J_{r,r+1} = -\tfrac{1}{2}[J + \alpha(u_r - u_{r+1})], \tag{1}$$

where, g is the Holstein e-ph coupling in *energy* units, α is the SSH e-ph coupling in units energy$\times$length^{-1}, J is the nearest neighbors hopping integral for an undistorted chain, $f_r^\dagger$ and f_r create and destroy electrons on the r-lattice site, u_r is the displacement of the rth atomic group along the molecular axis, $b_r^\dagger$ and b_r are the real space creation and annihilation phonon operators. The noninteracting phonon Hamiltonian H_{ph} is assumed to be given, in both models, by a set of independent oscillators. Taking ω as the characteristic phonon energy, the displacement field can be written as $u_r=(2M\omega)^{-1/2}(b_r^\dagger+b_r)$ and H^H transforms into

$$H^H = -\frac{J}{2}\sum_r (f_r^\dagger f_{r+1} + f_{r+1}^\dagger f_r) + \overline{g}\sum_r u_r f_r^\dagger f_r,$$

$$\overline{g} = g\sqrt{2M\omega}, \tag{2}$$

with $\overline{g}$ dimensionally equivalent to the coupling α of the SSH model. Choosing the atomic mass M of order 10^4 times the electron mass, we get $\overline{g}\simeq 1.1456\times g\sqrt{2\omega}$[meV Å^{-1}] where g is given in units of ω and the latter is given in meV. This transformation allows us to compare numerically the e-ph effective coupling in the two Hamiltonian models.

Let us apply to the Hamiltonians in Eq. (1) space-time mapping techniques previously used i.e., in the path integral formulation of the theory of dilute magnetic alloys[28] and in the path integral study of A15 compounds with strong electron-phonon coupling.[29]

Thus, we introduce $x(\tau)$ and $y(\tau')$ as the electron coordinates at the r and $r+1$ lattice sites, respectively, while the spatial e-ph correlations contained in (1) are mapped onto the time axis by changing: $u_r\rightarrow u(\tau)$ and $u_{r+1}\rightarrow u(\tau')$. Then, H^H in (2) and H^{SSH} in (1) transform to

$$H^H(\tau,\tau') = -\frac{J}{2}(f^\dagger(x(\tau))f(y(\tau')) + f^\dagger(y(\tau'))f(x(\tau))) + \overline{g}u(\tau)f^\dagger(x(\tau))f(x(\tau)),$$

$$H^{\mathrm{SSH}}(\tau,\tau') = J_{\tau,\tau'}(f^\dagger(x(\tau))f(y(\tau')) + f^\dagger(y(\tau'))f(x(\tau))),$$

$$J_{\tau,\tau'} = -\tfrac{1}{2}[J + \alpha(u(\tau) - u(\tau'))]. \tag{3}$$

τ and τ' are continuous variables ($\in[0,\beta]$) in the Matsubara Green's functions formalism with β being the inverse temperature hence, the electron hops are not constrained to first neighbors sites along the chain. Accordingly, the Hamiltonians in (3) are more general than the real space Hamiltonians in (1). Note that, while the Holstein model assumes a local e-ph interaction along the τ-axis, in the SSH picture the electron hopping is accompanied by a time dependent displacement of the atomic coordinate.

The ground state of the SSH Hamiltonian is twofold degenerate and, in real space, a soliton connects the two phases with different senses of dimerization. As a localized electronic state is associated to the soliton the SSH model describes in principle both electron hopping between solitons and thermally activated hopping to band states. By mapping onto the τ-axis we introduce time dependent electron hops while maintaining the fundamental features of the SSH Hamiltonian. Equations (3) display the semiclassical nature of our method in which quantum mechanical degrees of freedom interact with the classical variables $u(\tau)$. After setting $\tau'=0$, $u(0)\equiv y(0)\equiv 0$, we take the thermal averages for the electron operators over the ground states of the respective Hamiltonians thus obtaining the average energies per lattice site due to electron hopping plus e-ph coupling:

$$\frac{\langle H^H(\tau)\rangle}{N} = -\frac{J}{2}G^{\pm}[x(\tau),\tau] + \overline{g}u(\tau),$$

$$\frac{\langle H^{\mathrm{SSH}}(\tau)\rangle}{N} = -\left(\frac{J}{2} + \alpha u(\tau)\right)G^{\pm}[x(\tau),\tau],$$

$$G^{\pm}[x(\tau),\tau] = G[-x(\tau),-\tau] + G[x(\tau),\tau] = \frac{2a}{\pi}\int_0^{\pi/a} dk\,\cos[kx(\tau)]\cosh(\varepsilon_k\tau)n_F(\varepsilon_k), \tag{4}$$

where N is the number of lattice sites, $G[x(\tau),\tau]$ is the electron propagator, a is the lattice constant, $\varepsilon_k=-(J/2)\cos(ka)$, and $n_F(\varepsilon_k)$ is the Fermi function.

In general, the phonon partition function perturbed by a source current $j(\tau)$ can be expanded in anharmonic series as

$$Z_{\mathrm{ph}}[j(\tau)] \simeq Z_h\left(1 + \sum_{l=1}^{k}(-1)^l\langle C^l\rangle_{j(\tau)}\right),$$

$$Z_h = \prod_{i=1}^{N}\frac{1}{2\sinh(\omega_i\beta/2)}, \tag{5}$$

where the cumulant terms $\langle C^l\rangle_{j(\tau)}$ are expectation values of powers of correlation functions of the perturbing current. The averages are meant over the ensemble of the N harmonic oscillators (having energies ω_i) whose partition function is Z_h. As the oscillators are decoupled we study the anharmonicity induced on a single oscillator with energy ω by the source currents peculiar of the Hamiltonians in (3). Being, $j^H(\tau)=\overline{g}u(\tau)$ and $j^{\mathrm{SSH}}(\tau)=-\alpha u(\tau)G^{\pm}[x(\tau),\tau]$ we get

$$\langle C^k\rangle_{jH} = \frac{Z_h^{-1}}{k!}\oint Du(\tau)\left[\bar{g}\int_0^\beta d\tau u(\tau)\right]^k \times\exp\left[-\int_0^\beta d\tau\frac{M}{2}(\dot{u}^2(\tau)+\omega^2u^2(\tau))\right],$$

$$\langle C^k\rangle_{j\mathrm{SSH}}(x) = \frac{Z_h^{-1}}{k!}\oint Du(\tau)\left[-\alpha\int_0^\beta d\tau u(\tau)G^{\pm}[x(\tau),\tau]\right]^k \times\exp\left[-\int_0^\beta d\tau\frac{M}{2}(\dot{u}^2(\tau)+\omega^2u^2(\tau))\right]. \quad (6)$$

As a direct consequence of the time retardation in the SSH e-ph interactions, the SSH cumulant series turns out to depend on the electron path coordinates.

In order to calculate Eqs. (6), we expand the periodic oscillator path ($u(\tau+\beta)=u(\tau)$) in N_F Fourier components

$$u(\tau) = u_o + \sum_{n=1}^{N_F} 2(\Re u_n\cos(\omega_n\tau) - \Im u_n\sin(\omega_n\tau))$$

$$\omega_n = 2\pi n/\beta, \quad (7)$$

and choose a measure of integration which normalizes the kinetic term in the oscillator field action

$$\oint Du(\tau) \equiv \frac{\sqrt{2}}{(2\lambda_M)^{2N_F+1}}\int_{-\infty}^{\infty}du_o\prod_{n=1}^{N_F}(2\pi n)^2\int_{-\infty}^{\infty}d\Re u_n\int_{-\infty}^{\infty}d\Im u_n,$$

$$\oint Du(\tau)\exp\left[-\frac{M}{2}\int_0^\beta d\tau\dot{u}^2(\tau)\right]\equiv 1, \quad (8)$$

being $\lambda_M=\sqrt{\pi\hbar^2\beta/M}$.

As $\int_0^\beta d\tau u(\tau)=\beta u_0$, using Eqs. (7) and (8), the Holstein cumulant series can be worked out analytically as a function of the cutoff N_F. The first of Eqs. (6) gets

$$\langle C^k\rangle_{jH}^{N_F} = \frac{Z_h^{-1}}{k!}\frac{(\bar{g}\beta\lambda_M)^k(k-1)!!}{\pi^{k/2}(\omega\beta)^{k+1}}\prod_{n=1}^{N_F}\frac{(2n\pi)^2}{(2n\pi)^2+(\omega\beta)^2}, \quad (9)$$

where only even k terms survive. As the cumulants should be stable against the number of Fourier components in the oscillator path expansion we set the minimum N_F through the condition $2N_F\pi\gg\omega\beta$. Since the Holstein source current does not bear any dependence on the electron path coordinates, the Holstein expansion in Eq. (9) coincides with the cumulant series for a time averaged electron particle path.[27]

To compute the second of Eqs. (6), we expand also the electron path under the closure condition $x(\tau+\beta)=x(\tau)$:

$$x(\tau) = x_o + \sum_{m=1}^{M_F} 2(\Re x_m\cos(\omega_m\tau) - \Im x_m\sin(\omega_m\tau)),$$

$$\omega_m = 2\pi m/\beta, \quad (10)$$

with, in general, $M_F\neq N_F$. Thus, the general cumulant term is obtained by averaging the second of Eqs. (6) over a set of electron particle paths:

$$\langle C^k\rangle_{j\mathrm{SSH}} = \sum_{x_o,\Re x_m,\Im x_m}\langle C^k\rangle_{j\mathrm{SSH}}(x). \quad (11)$$

Two Fourier components ($M_F=2$) suffice to get numerical convergence in Eq. (11). We point out that, the computation of the anharmonic expansion in the SSH model requires for any choice of electron path coefficients, double summations over Brillouin zone [see Eq. (4)], and inverse temperature (τ) values [see the second of Eqs. (6)].

III. PHONON THERMODYNAMICS

The phonon thermodynamics can be derived from Eq. (5) via computation of the phonon free energy $F^{(k)}(T) = -\beta^{-1}\ln[Z_{\mathrm{ph}}[j(\tau)]]$.

To proceed one needs a criterion to find the temperature dependent cutoff k^* in the cumulant series. We feel that, in the low T limit, the third law of thermodynamics may offer the suitable constraint to determine k^*. Then, set the input parameters α (g in the Holstein model), J and ω, the program searches for the cumulant order such that phonon entropy $E_V^{(k)}(T)$ and heat capacity $C_V^{(k)}(T)$ vanish in the zero temperature limit. In a constant volume transformation, we compute

$$E_V^{(k)}(T) = -[F^{(k)}(T+2\Delta) - 2F^{(k)}(T+\Delta)]/\Delta,$$

$$C_V^{(k)}(T) = -[F^{(k)}(T+2\Delta) - 2F^{(k)}(T+\Delta) + F^{(k)}(T)] \times\left(\frac{1}{\Delta}+\frac{T}{\Delta^2}\right), \quad (12)$$

Δ being the incremental step and k^* is determined, at finite T, as the minimum value for which the anharmonic cumulant series converges with an accuracy of 10^{-4}. The results are displayed in Fig. 1 for the case of a low energy oscillator and a narrow band hopping integral, $J=0.1$ eV. Three values of α are assumed to emphasize the dependence of the SSH model thermodynamics on the e-ph coupling. The $g=3$ value for the Holstein model calculations yields a $\bar{g}$ coincident with the largest $\alpha=21.74$ meV Å^{-1}.

The Holstein cumulant expansion causes a slight and slope preserving lowering of the phonon free energy with respect to the harmonic plot. As a consequence the Holstein entropy and heat capacity, computed via Eqs. (12), are superimposed to the harmonic quantities. However, looking at Fig. 1(d) (case $g=3$), we see that a large number of cumulant terms is required to get convergence in the Holstein series as the cutoff k^* markedly grows below 80 K, attaining the value $k^*=40$ at $T=1$ K. Thus, e-ph anharmonicities strongly renormalize the Holstein partition function, essentially stabilize the system, but there is no trace of anharmonicity in the

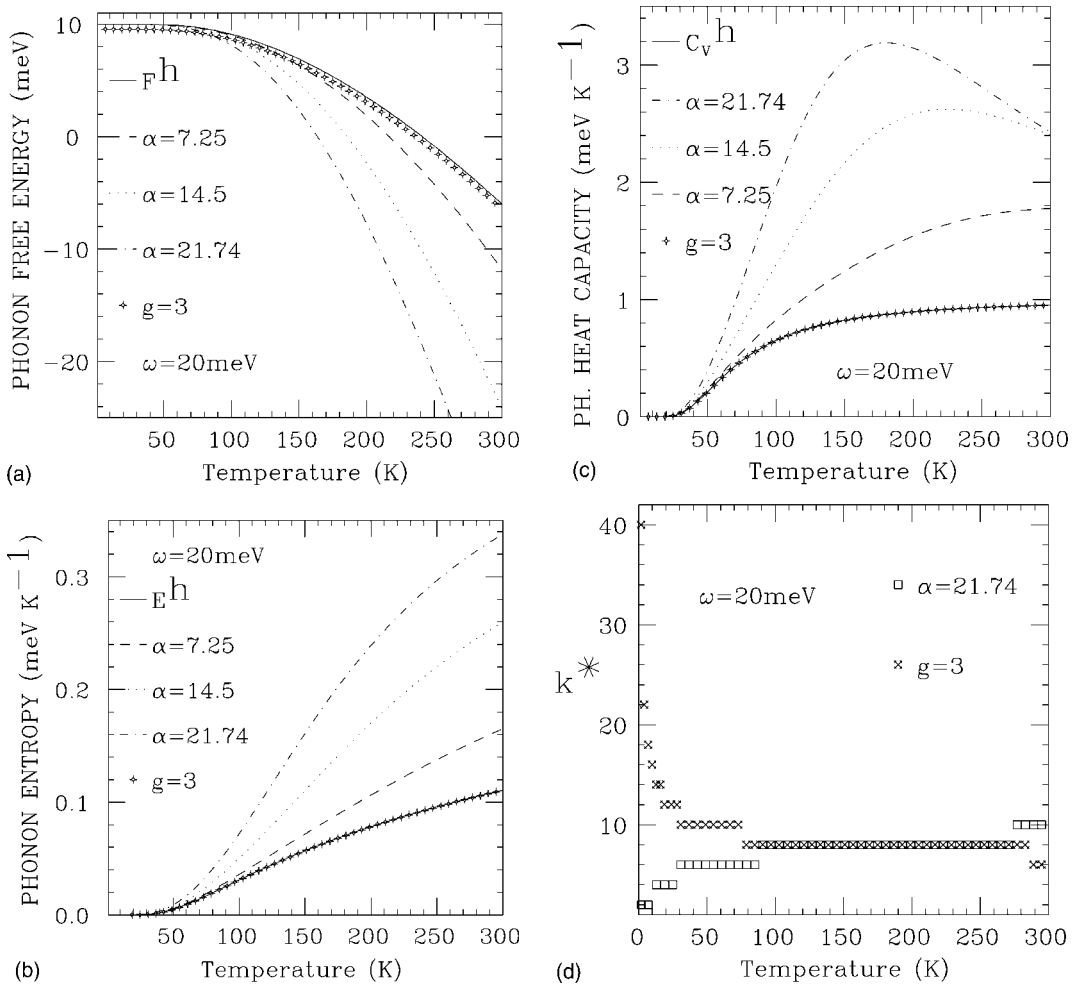

FIG. 1. Phonon (a) free energy, (b) entropy, and (c) heat capacity versus temperature in the Su-Schrieffer-Heeger model with e-ph anharmonic contributions due to three values of the coupling α in units meV Å^{-1}. The Holstein model results are computed for the coupling g (in units of ω) corresponding to the largest of the three α values. Also the harmonic phonon functions are plotted for comparison. (d) Number of anharmonic terms in the cumulant series yielding convergent thermodynamical quantities versus temperature both in the Su-Schrieffer-Heeger model (α case) and in the Holstein model (g case). A low energy oscillator is assumed.

phonon free energy temperature derivatives.[30]

Much different is the trend of the anharmonic corrections in the SSH model. The main features can be summarized as follows: (i) the phonon free energy [Fig. 1(a)] and its derivatives [Figs. 1(b) and 1(c)] largely deviate from the harmonic plots and strongly depend on α; (ii) there is a threshold α value above which the heat capacity displays a peak. By enhancing α [Fig. 1(c)] the height of the peak grows and the bulk of the anharmonic effects on the heat capacity is shifted towards lower T; (iii) at high T the anharmonic corrections renormalize downwards the phonon free energy but their effect on the heat capacity tends to decrease signaling that e-ph nonlinearities are rather to be seen in the intermediate temperature range. Note that the size of the anharmonic enhancement is about a factor 4 larger than the value of the harmonic oscillator heat capacity at $T \sim 170$ K; (iv) the cutoff k^* in the SSH model [Fig. 1(d)] attains the value 10 at room temperature while the cumulant series converges with a low number of terms ($k^*=2$) at low T. At intermediate $T \in [90,270]$, the SSH cutoff overlaps the Holstein cutoff at the value $k^*=8$.

The location of the heat capacity peak along the temperature axis strongly varies with the oscillator energy. In Fig. 2 we select two energy values and report the crossover temperatures for a set of e-ph coupling strengths. By increasing ω at fixed α the peak shifts towards high T and it shows up above a minimum α whose value increases at larger ω. Thus, higher energy oscillators are more stable against e-ph induced anharmonicity since larger couplings are required to introduce signatures of nonlinear behavior in the phonon heat capacity.

So far we have focused on the thermodynamics of the phonon subsystem. The question arises whether and to which extent the *anharmonic phonon* heat capacity affects the *total* heat capacity of the SSH model. As discussed in Ref. 26 the total heat capacity is given by the phonon contribution plus a source heat capacity which includes both the electronic contribution (related to the electron hopping integral) and the contribution due to the source action [the latter being $\propto \alpha^2$, see Eqs. (6) in Ref. 26]. A bath of harmonic phonons has been assumed in our previous work. Now we compare the

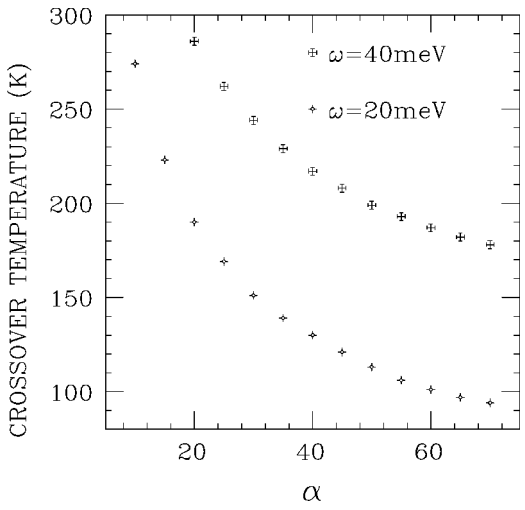

FIG. 2. Temperature locations of the peak in the Su-Schrieffer-Heeger phonon heat capacity versus e-ph coupling in units meV Å^{-1}.

anharmonic phonon heat capacity (C_V^{anh}) and the source heat capacity, here termed $C_V^{e\text{-}p}$ to emphasize the dependence both on the electronic and on the e-ph coupling terms. The plot displaying the largest peak in Fig. 1(c) is reported on in Fig. 3(a) while $C_V^{e\text{-}p}$ is computed according to the method described in Ref. 26 after setting $\alpha=21.74$ meV Å^{-1}. Also the total heat capacity ($C_V^{\mathrm{tot}}=C_V^{\mathrm{anh}}+C_V^{e\text{-}p}$) is shown in Fig. 3(a). At low temperatures, $C_V^{e\text{-}p}$ yields the largest effect mainly due to the electronic hopping while at high T, $C_V^{e\text{-}p}$ prevails as the source action becomes dominant. In the intermediate range ($T\in[90,210]$) the anharmonic phonons provide the highest contribution although their characteristic peak is substantially smeared in the total heat capacity by the source term background. Figure 3(b) compares C_V^{anh} and $C_V^{e\text{-}p}$ for two increasing values of α: while the anharmonic peak shifts downwards (along the T axis) by enhancing α, C_V^{anh} remains larger than $C_V^{e\text{-}p}$ in a temperature range which progressively shrinks due to the strong dependence of the source action on the strength of the e-ph coupling. Finally, it has to be pointed out that the low temperature upturn displayed in the *total heat capacity over T* ratio[26] is not affected by the inclusion of phonon anharmonic effects which tend to become negligible at low temperatures.

IV. FINAL REMARKS

The Holstein and the Su-Schrieffer-Heeger Hamiltonian present a fundamental difference with respect to the nature of the e-ph coupling. Mapping the real space interactions onto the time scale we have shown that the Holstein e-ph interactions are *local* in time while, in the SSH model, the electronic hopping induces a time dependent lattice displacement thus leading to a *nonlocal* e-ph coupling. As a consequence the source current peculiar of the SSH model depends both on time and on the electron path coordinates. We have applied the path integral method to analyse the perturbing effects of the source currents (in both models) on the phonon subsystems by expanding the phonon partition function in

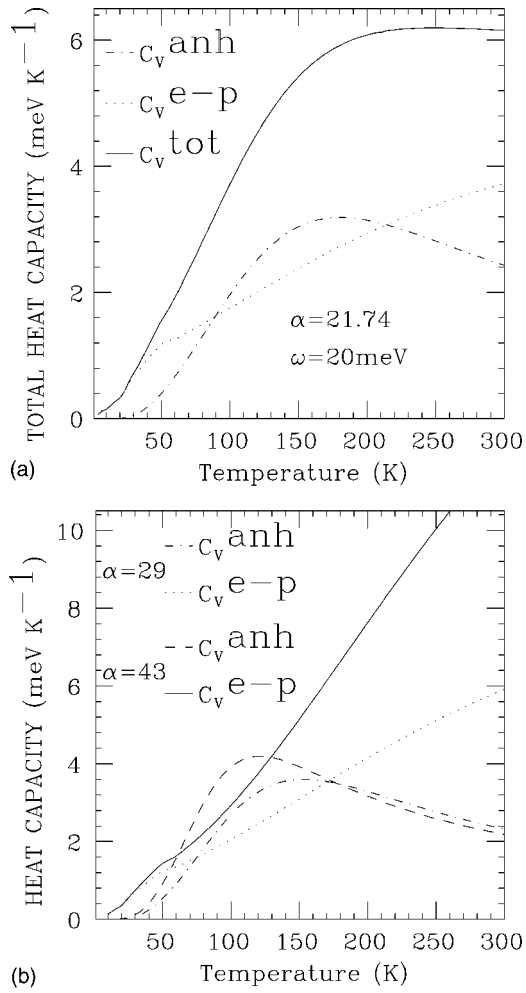

FIG. 3. (a) Total heat capacity versus temperature in the Su-Schrieffer-Heeger model. The contributions due to anharmonic phonons (C_V^{anh}) and electrons plus electron-phonon interactions ($C_V^{e\text{-}p}$) are plotted separately. The largest α of Fig. 1 is assumed. (b) C_V^{anh} and $C_V^{e\text{-}p}$ for two values of α in units meV Å^{-1}. $\omega=20$ meV.

cumulant series. In the low temperature limit, the constraint imposed by the third law of thermodynamics permits us to determine the cutoff k^* in the anharmonic expansion: while the SSH series converges rapidly, a high number of cumulants is required in the Holstein model to stabilize the low T equilibrium properties. At intermediate and high T, $k^*(T)$ is comparable in both models. However, looking at the behavior of the thermodynamic properties we find striking differences between the two models. The Holstein phonon heat capacity does not show any trace of anharmonicity induced by the e-ph coupling while the SSH phonon heat capacity exhibits a peak whose location along the T axis strongly depends on the strength of the coupling α. By increasing α at a fixed T, k^* grows and the phonon partition function becomes larger. As a result the point of *most rapid decrease* in the SSH phonon free energy versus temperature shifts downwards and the associated heat capacity peak is found at lower T. At high temperatures the free energy decreases regularly and the anharmonic effects on the heat capacity are reduced. Infact, at high T, the time (τ) retardation between electron hopping and atomic displacement is shortened as τ encoun-

ters the upper limit of a small inverse temperature.

Finally, we have computed the general path integral in the SSH model for an electron path moving in a bath of anharmonic oscillators. We have derived the total heat capacity and pointed out the contribution of the anharmonic phonon with respect to the purely electronic and e-ph terms. The anharmonic effects are relevant in the intermediate temperature range whereas the peak is smeared by the electronic hopping term (on the low temperature side) and by the source action heat capacity at high temperatures.

*Electronic address: marco.zoli@unicam.it

[1] H. Falk, Am. J. Phys. **38**, 858 (1970).
[2] K. Michielsen and H. de Raedt, Z. Phys. B: Condens. Matter **103**, 391 (1997).
[3] J.C.K. Hui and P.B. Allen, J. Phys. C **8**, 2923 (1975).
[4] T.H.K. Barron, in *Lattice Dynamics*, edited by R.F. Wallis (Pergamon, Oxford, 1965).
[5] M. Zoli, Phys. Rev. B **41**, 7497 (1990).
[6] T. Holstein, Ann. Phys. (N.Y.) **8**, 325 (1959).
[7] W.P. Su, J.R. Schrieffer, and A.J. Heeger, Phys. Rev. Lett. **42**, 1698 (1979); A.J. Heeger, S. Kivelson, J.R. Schrieffer, and W.-P. Su, Rev. Mod. Phys. **60**, 781 (1988).
[8] A.S. Alexandrov and N.F. Mott, Rep. Prog. Phys. **57**, 1197 (1994).
[9] Yu Lu, *Solitons and Polarons in Conducting Polymers* (World Scientific, Singapore, 1988).
[10] V.M. Stoianović, P.A. Bobbert, and M.A.J. Michels, Phys. Rev. B **69**, 144302 (2004).
[11] C.A. Perroni, E. Piegari, M. Capone, and V. Cataudella, Phys. Rev. B **69**, 174301 (2004).
[12] D.K. Campbell and A.R. Bishop, Phys. Rev. B **24**, 4859 (1981).
[13] S. Stafström and K.A. Chao, Phys. Rev. B **30**, 2098 (1984).
[14] N. Miyasaka and Y. Ono, J. Phys. Soc. Jpn. **70**, 2968 (2001).
[15] M. Zoli, Phys. Rev. B **66**, 012303 (2002).
[16] N.K. Voulgarakis and G.P. Tsironis, Phys. Rev. B **63**, 014302 (2001).
[17] Y. Zolotaryuk, P.L. Christiansen, and J.J. Rasmussen, Phys. Rev. B **58**, 14305 (1998).
[18] T.D. Holstein and L.A. Turkevich, Phys. Rev. B **38**, 1901 (1988).
[19] H.-B. Schüttler and T.D. Holstein, Phys. Rev. Lett. **51**, 2337 (1983).
[20] D. Emin, Phys. Rev. Lett. **72**, 1052 (1994); Phys. Status Solidi B **218**, 259 (2000).
[21] J.K. Freericks and G.D. Mahan, Phys. Rev. B **54**, 9372 (1996).
[22] J. Zhong and H.-B. Schüttler, Phys. Rev. Lett. **69**, 1600 (1992).
[23] M. Zoli and A.N. Das, J. Phys.: Condens. Matter **16**, 3597 (2004).
[24] R.P. Feynman, Phys. Rev. **97**, 660 (1955).
[25] H. Kleinert, *Path Integrals in Quantum Mechanics, Statistics and Polymer Physics* (World Scientific, Singapore, 1995).
[26] M. Zoli, Phys. Rev. B **67**, 195102 (2003).
[27] M. Zoli, J. Phys.: Condens. Matter **15**, 6239 (2003).
[28] D.R. Hamann, Phys. Rev. B **2**, 1373 (1970).
[29] C.C. Yu and P.W. Anderson, Phys. Rev. B **29**, 6165 (1984).
[30] V.L. Gurevich, D.A. Parshin, and H.R. Schober, Phys. Rev. B **67**, 094203 (2003).